An Electrochemical Impedance-Based Thermal Flow Sensor for Physiological Fluids

Alex Baldwin, Lawrence Yu, and Ellis Meng, *Senior Member, IEEE*

***Abstract*— A novel electrochemical-thermal flow sensor was developed for use in physiological liquids. The sensor was constructed out of a platinum resistive heater and platinum sensing electrodes on a Parylene C substrate, rendering it flexible and fully biocompatible. During heating, changes in electrochemical impedance across the sensing electrodes were used to detect changes in temperature, and highly sensitive flow measurements were achieved with overheat temperatures of only 1 °C. The sensor's biocompatibility and low overheat temperature make it an ideal candidate for chronic *in vivo* applications. [2016-0170]**

***Index Terms*— Bioimpedance, impedance, biomedical transducers, microelectronic implants, *in vivo*, fluid flow, microfluidics, fluid flow measurement, electrothermal effects, temperature dependence, Parylene C, thermal flow sensing, electrochemical-microelectromechanical systems (EC-MEMS).**

I. Introduction

PRECISE and accurate knowledge of flow rate is a ubiquitous concern of both medicine and biology. Accurate flow measurement is critical in applications such as drug delivery, drug synthesis, and diagnostic tests. For *in vivo* applications, implantable microscale flow sensors have been proposed to monitor the flow of blood, cerebrospinal fluid, or other bodily fluids, provide tracking of a disease state, or deliver diagnostic information to clinicians. However, few flow sensors possess all the capabilities necessary for medical applications, which include compatibility with physiological fluid, low detection limit, low power consumption, and biocompatibility for *in vivo* implantation. Mechanical designs, which often mimic macroscale turbine or cantilever flow sensors [6], possess moving parts at risk of biofouling when exposed to biological fluids. Thus, designs having no moving parts are preferred for physiological environments.

Microfluidic *thermal* flow sensors have been successfully used for gas and liquid sensing in several applications and operate by measuring convective heat transfer in a fluid as a function of flow rate [1]. Although many microfabricated thermal flow sensors have been successfully developed and commercialized for gas flow, there are additional challenges involved in designing sensors for *in vivo* measurement of physiological liquids. Due to the high thermal conductance of water and physiological fluids, sensors must be smaller and operate at a higher overheat temperature to minimize heat dissipation losses. Sensors designed for implantation must also minimize heating to avoid damaging the body, and must be constructed from biocompatible materials that will not corrode or degrade *in vivo.* Most prior reports of microfabricated thermal flow sensors employ traditional semiconductor-based materials, typically as silicon-based sensors employing a thin-film microheater (often relying on silicon nitride membranes for thermal isolation) with joule heaters and resistance temperature detectors (RTDs) fabricated from polysilicon [7]–[9], germanium [11]–[13], or metals [15]. These sensors have achieved high accuracies and sensitivities over a wide range of flow velocities thanks to the high temperature sensitivity of doped polysilicon and germanium, but are not suitable for chronic implantation due to their corrosion under chronic exposure to physiological fluid [17]. Some sensors, designed for use in water or physiological fluids, have been reported with metal heaters and temperature sensors fabricated on polyimide [14], [18], Parylene C [10], [19], [20], or other biocompatible polymer substrates [16], [21]. Unfortunately, metals have an order of magnitude lower sensitivity to temperature changes than semiconductor-based resistors, resulting in low sensitivity and requiring high overheat temperatures.

The low sensitivity of current polymer-based thermal flow sensors and the lack of biocompatibility in semiconductor-based thermal flow sensors has left a need for a flow sensor which is both highly sensitive and biocompatible in design and material. We have developed a thermal flow sensor designed not only to function in physiological fluids, but to exploit the ionic conductivity of several biological liquids which enables improved sensitivity. Temperature-mediated changes in the conductivity of the solution are monitored via high-frequency electrochemical impedance to deduce flow rate, and the corresponding temperature sensitivity is an order of magnitude larger than the temperature coefficient of resistance (TCR) in metallic RTDs (Table 1). The new sensor is constructed of a platinum resistive heater and sensing electrodes on a thin film Parylene C substrate. Parylene's high thermal resistivity reduces thermal conduction across the substrate. A time-of-flight method for flow transduction was developed which measures the rate of heat transfer due to both diffusion and convection, enabling accurate measurements of low flow rates

Manuscript received July 22, 2016; revised September 7, 2016; accepted September 16, 2016. Date of publication October 13, 2016; date of current version November 29, 2016. This work was supported in part by the University of Southern California Coulter Translation Research Partnership Award and in part by NSF under Award ECCS-1231994 and Award EFRI-1332394. Subject Editor A. Zhang.

A. Baldwin and L. Yu are with the Biomedical Engineering Department, University of Southern California, Los Angeles, CA 90089 USA (e-mail: abbaldwi@usc.edu; lawrence.yu@usc.edu).

E. Meng is with the Biomedical Engineering and the Electrical Engineering Department, University of Southern California, Los Angeles, CA 90089 USA (e-mail: ellis.meng@usc.edu).

Color versions of one or more of the figures in this paper are available online at http://ieeexplore.ieee.org.

Digital Object Identifier 10.1109/JMEMS.2016.2614664

TABLE I
TEMPERATURE COEFFICIENT OF RESISTANCE (TCR) OF METALS AND SEMICONDUCTORS WHICH ARE COMMONLY USED IN RESISTIVE TEMPERATURE SENSORS, AS WELL AS SEVERAL IONIC SOLUTIONS INCLUDING HUMAN CEREBROSPINAL FLUID [1]–[3]

Material	TCR (%/ºC)
Platinum	0.392
Copper	0.430
Gold	0.390
Polysilicon	-2.5 to 0.1
Germanium	-2.0
1.32M (5%) NaOH	-2.01
7.9M (30%) NaOH	-4.50
2.95M (20%) KCl	-1.68
Human Cerebrospinal Fluid	-1.98

and bidirectional flow detection using only a single temperature sensor. Here we present the operating theory, fabrication, and characterization of the sensor and sensing mechanism.

II. THEORY

A. Electrolyte Conductivity

The conductance, and thus the electrochemical impedance, of an aqueous electrolyte solution is highly dependent on temperature. Electrical conduction through an electrolyte solution arises from the movement of charged ions, and the solution's ionic conductance describes the movement of these ions in an electric field. This movement is determined by the sum of forces between ions and the surrounding solution. Bulk conductance is directly proportional to ionic concentration but a molar conductivity can be defined as $\Lambda = G/c$, where G is the bulk conductance, and c is the molarity of ions [22]. The limit of conductivity as concentration goes to zero is known as the state of 'infinite dilution' and is useful to consider since in this state, conductivity depends on interactions between a single ion and the solution. If the mobility of an ion is defined as the limiting velocity per applied force, the conductivity at infinite dilution is

$$\lambda_0 = uqF \tag{1}$$

where u is ionic mobility, q is the charge on the ion, and F is Faraday's constant [23]. Stoke's law gives the first approximation for ionic mobility as a product of the drag between a spherical ion and a continuous solution, and this law can be extended by including dielectric losses produced by moving charges to give

$$u^{-1} = 4\pi\eta r + \frac{3}{8}q^2\frac{\varepsilon_0 - \varepsilon_\infty}{\varepsilon_0^2 r^3}\tau_0 \tag{2}$$

where η is water's viscosity, r is ionic radius, ε_0 and ε_∞ are the high-frequency and low-frequency limits of the solution permittivity, and τ_0 is the Debye relaxation time [24].

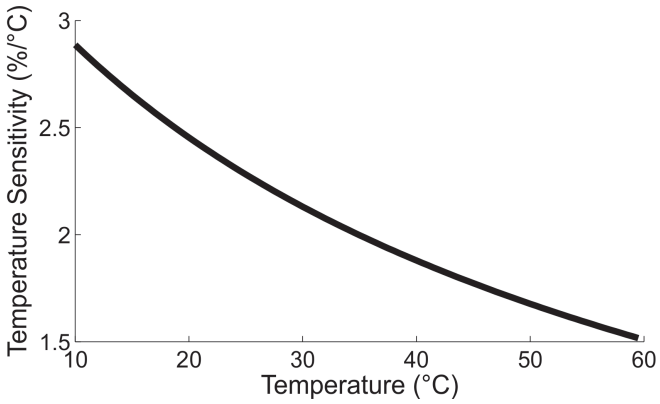

Fig. 1. Temperature sensitivity of conductivity, which is comparable to TCR, of an aqueous solution of sodium ions at infinite dilution.

All temperature-dependent terms in this expression are parameters of water, and viscosity is the term which has the largest effect, indicating that the effect of changing temperatures on ionic mobility is largely independent of the ionic species present and is closely related to changes in water's viscosity.

Viscosities, permittivities, and Debye relaxation times of water at temperatures from 10-60°C were used to calculate conductivity at infinite dilution of a common ion (sodium) [25]–[27]. Figure 1 shows the percent change in this conductivity per °C, which is equivalent the temperature sensitivity of the solution analogous to TCR of a solid.

The temperature coefficient of conductivity at infinite dilution is a good indicator of the response of an electrolyte solution to changes in temperature, but forces exist between ions that must be taken into account for real solutions. Debye, Huckel, and Onsager summarize these forces in the expression

$$\Lambda = \Lambda^0 - \left(\frac{z^2eF^2}{3\pi\eta\left(\frac{2}{\varepsilon RT}\right)^{\frac{3}{2}}} + \frac{qz^3eF}{24\pi\varepsilon RT\sqrt{\frac{2}{\varepsilon RT}}}\Lambda^0\right)\sqrt{c} \tag{3}$$

where c is the electrolyte concentration in moles per liter, Λ^0 is the infinite dilution conductivity, z is the valency number of each ionic species, R is the gas constant, e is the electron charge, and q describes the symmetry of an ionic species [28]. Calculating this conductivity for various ionic species reveals that the temperature coefficient of conductivity decreases as concentration increases. However, the difference in temperature coefficient between infinite dilution and most physiological fluids is minimal. For example, cerebrospinal fluid and blood have approximate ionic molarities of 295 mM [29] and 345 mM [30], which have a difference in temperature coefficient from a solution at infinite dilution of 0.19% and 0.21% respectively.

Changes in conductivity of an electrolyte solution can be detected by measuring the electrochemical impedance between two immersed electrodes. Typically, three electrodes are used for electrochemical measurements, with one electrode providing a stable reference voltage in the electrolyte. This allows for sensitive measurements at the electrode-electrolyte interface and has been used for a number of amperometric-based sensors. However, to measure changes in the bulk

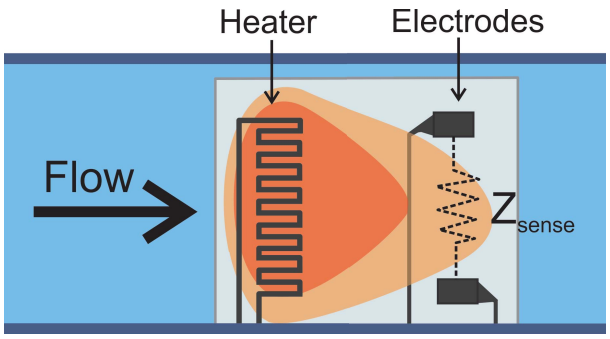

Fig. 2. Our sensor transduces flow through the transfer of heat from a resistive heater to flowing fluid and from the fluid to a pair of electrodes. The electrodes sense changes in temperature via changes in electrochemical impedance (Z_{sense}). Orange represents the temperature distribution being distorted by flow, blue represents the flowing liquid and light blue represents the polymer substrate.

conductivity of the electrolyte a high frequency signal is passed between electrodes, and at the proper frequency the electrode-electrolyte interface is completely bypassed and a reference electrode is no longer necessary.

B. Flow Measurement

To enable bidirectional flow measurement at low flow rates, a time of flight method was developed requiring a heater and a single pair of impedance electrodes, where the rate at which the heated solution reaches the electrodes is used to transduce flow velocity. Figure 2 shows the basic setup of our sensor.

The transfer of heat away from a heater can be described using the convection-diffusion equation:

$$\frac{\partial T}{\partial t} = \nabla * (\alpha \nabla T) - \nabla * (\mathrm{VT}) + H(x,t) \tag{4}$$

where T is temperature, α is the fluid's thermal diffusivity, V is the fluid's velocity vector at any point, and $H(x, t)$ is any change in temperature forced upon the system [31]. The impulse response to the convection-diffusion equation is a constantly widening and shifting Gaussian curve, and when convection is the dominant method of heat transfer, the peak of this Gaussian can be tracked to derive the flow velocity. However, for low flow rates and over short distances, diffusion is the dominant method of heat transfer, and the Gaussian will tend to dissipate before the peak moves a significant distance. The relative dominance of convection over diffusion is described by the Peclet number

$$Pe = \frac{Lv}{\alpha} \tag{5}$$

where L is length and v is the scalar flow velocity [32]. When the Peclet number is greater than 1, the system is dominated by convection. The highest flow velocity we tested was around 800 μm/s, which with a temperature sensor spaced 1 mm away from the heater and using the thermal diffusivity of pure water ($\alpha = 143 \times 10^{-9}$ m^2/s) gives a Peclet number of 5.59. This indicates that the system is slightly convection-dominated but that reducing flow velocity would lead to a diffusion-dominated state. Therefore, a method of flow measurement is needed which operates in both diffusion-dominated and convection-dominated states.

The maximum rate of change of temperature at electrodes can be used to transduce flow velocity in both convection and diffusion-dominated states, since the heating profile around a heater is affected by both convection and diffusion. Measuring the maximum rate of change allows flow transduction down to arbitrarily low flow velocities and for both positive and negative flow directions. To validate this approach, a 1-dimensional finite difference simulation was used. Assuming perfect insulation and an infinitely long fluid cylinder, the explicit finite difference equation for heat transfer via the convection-diffusion equation in one dimension is

$$\frac{T_j^n - T_j^{n-1}}{\Delta t} = \alpha \frac{T_{j+1}^{n-1} - 2T_j^{n-1} + T_{j-1}^{n-1}}{(\Delta x)^2} - V \frac{T_{j+1}^{n-1} - T_{j-1}^{n-1}}{2\Delta x} + H \tag{6}$$

where T_j^n is the temperature at time $n\Delta t$ and position $j\Delta x$ [33]. The stability criteria for this method is $\Delta x < \frac{2\alpha}{V}$ and $\Delta t < \frac{\Delta x^2}{2\alpha}$. Choosing 50 μm for Δx and 5 ms for Δt satisfies these criteria. The initial temperature was set to 25 °C, and after 1 second, the heat at $x = 0$ increased by 2 °C to simulate constant current delivered to the heater. Heat conduction through the polymer substrate was considered to be negligible, since the polymer used (Parylene C) has a thermal conductivity an order of magnitude lower than the surrounding fluid (0.084 W/m·K, versus 0.596 W/m·K for water) [34].

Figure 3 shows the simulation results, which confirm that the heating profile 1 mm away from the heater is altered by changes in the flow velocity and that the maximum rate of change of temperature can be used to transduce flow. This method of flow transduction overcomes some limitations of traditional time of flight measurements and allows the temperature measurement electrodes to be placed close to the heater, allowing for smaller devices with lower overheat temperatures and enabling the accurate measurement of low flow velocities.

III. Sensor Design

Sensors which used the above principles to transduce flow velocity were designed and fabricated, each sensor consisting of a resistive heater and a pair of exposed platinum electrodes deposited on a thin-film Parylene C substrate, as show in Figure 4. The heater is 1 mm long and 250 μm wide and consists of a serpentine platinum trace with a trace width and spacing of 25 μm. Each heater has a DC resistance of 750-800 Ω, depending on process variations. The measurement electrodes are spaced 750 μm apart perpendicular to the direction of flow, with each electrode having a geometric surface area of 20000 μm^2. Two pairs of electrodes were fabricated on each sensor to enable accurate measurement over a large range of flow rates. Two different sensor variations were designed, one with electrodes spaced 0.5 mm and 2 mm away from the center of the heater and one with electrodes spaced at 1 mm and 3 mm. Each die also contained a previously reported pressure sensor [35] and patency sensor [36].

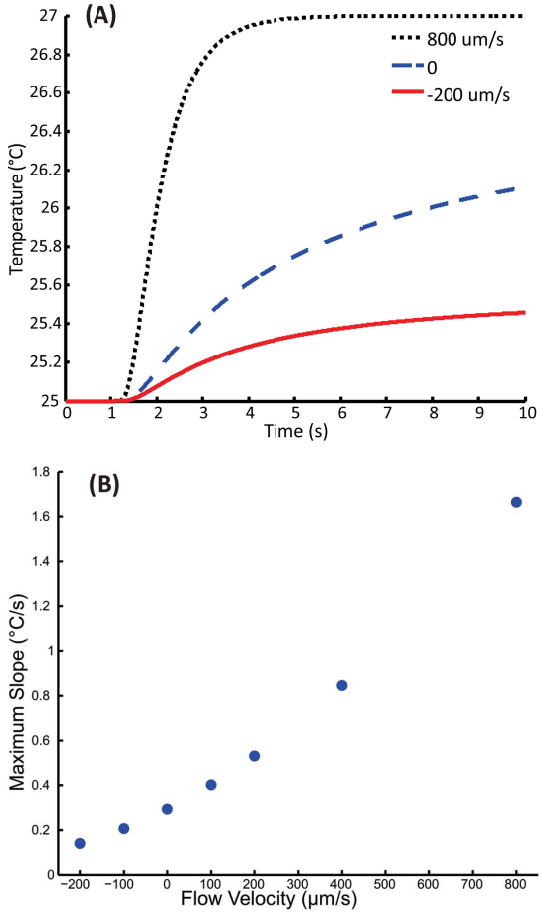

Fig. 3. (A) Simulations show that the temperature profile 1 mm away from the heater is dependent on flow and (B) that the maximum rate of change of temperature is related to flow velocity.

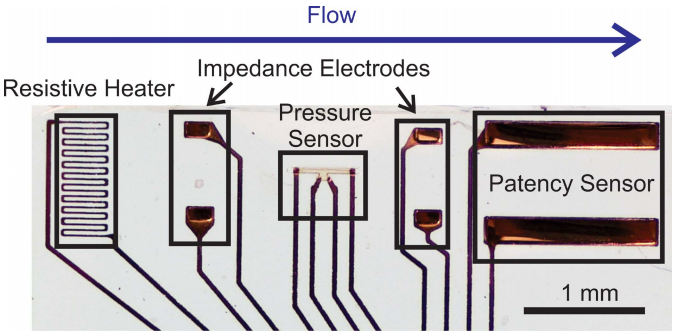

Fig. 4. Fabricated sensor die showing the resistive heater and two sets of impedance electrodes. The die also contains previously reported pressure and patency sensors.

IV. Fabrication

Fabrication followed previously reported surface micromachining processes for Parylene C MEMS devices described in detail elsewhere and briefly summarized here [37]. A 12 μm thick Parylene substrate was deposited on a silicon carrier wafer, and the heater, electrodes and contacts were defined in a single layer of 2000 Å thick sputtered platinum. Components were patterned with UV lithography followed by metal deposition and lift-off before being insulated in a second 12 μm thick Parylene layer. Electrode surfaces and contact pads were exposed using a switched chemistry deep reactive ion etching process in oxygen plasma and a second cutout etch was used to separate devices. The free-film devices were released from the carrier wafer by gently peeling while immersed in deionized water, and any residual photoresist was removed by washing in acetone.

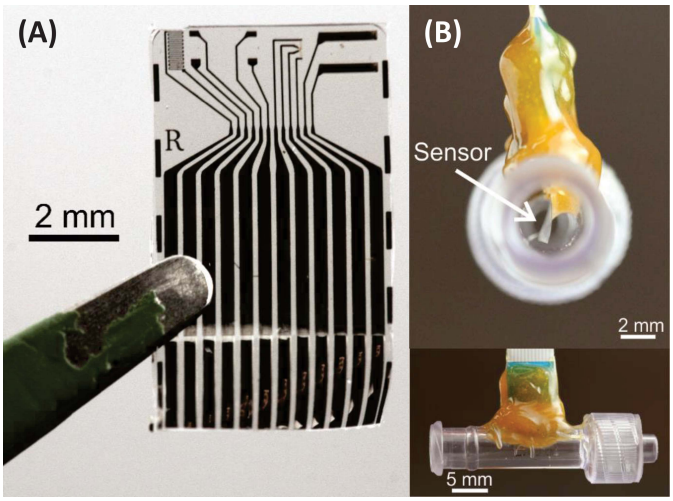

Fig. 5. A sensor die (A) just after being released from its silicon carrier wafer and (B) packaged in a luer lock connector for fluidic testing.

Electrical connections were made through a zero insertion force (ZIF) connector soldered onto a flat flexible cable. The contact pads of the released device were first attached to a 250 μm thick PEEK (polyetheretherketone) backing using cyanoacrylate glue to achieve the thickness necessary for insertion into the ZIF connector. The ZIF connector was then encapsulated with biocompatible EpoTek 353-NDT epoxy. For flow testing, the sensors were packaged into a luer lock, shown in Figure 5. Using a luer lock connector enables devices to easily attach to shunts and catheters currently used in hospitals, including external ventricular drains for cerebrospinal fluid, which is our primary target application. A slot was milled into the top of a luer lock connector with an inner diameter of 3.25 mm and the sensor was inserted and sealed with EpoTek 353-NDT epoxy such that one end of the sensor fixed to the connector and one free-standing. Care was taken to place the sensor films as close to the center of the luer lock connector as possible so that the resistive heater and electrodes are in the region of maximum flow velocity. An acrylic jig was used to hold the sensors in place while the epoxy dried.

V. Flow Testing and Characterization

The heater resistance and electrode impedance were characterized in phosphate-buffered saline (PBS), an isotonic solution commonly used to mimic solutions (pH 7.4, ionic molarity 280 mM), at temperatures between 25 and 50 °C. Tests were also performed in artificial cerebrospinal fluid (aCSF), which has a slightly higher ionic molarity and includes calcium and magnesium to better mimic the ionic environment in *in vivo*. aCSF was prepared by combining 8.66 g NaCl, 0.224 g KCl, 0.206 g $CaCl_2 \cdot 2H_2O$, 0.163 g $MgCl_2 \cdot 6H_2O$, 0.214 g $Na_2HPO_4 \cdot 7H_2O$, and 0.027 g

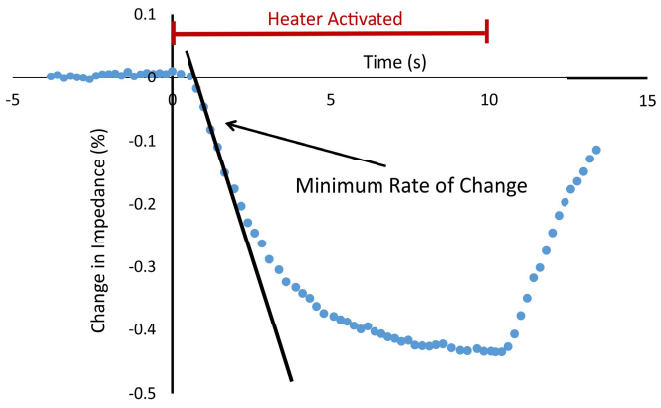

Fig. 6. To transduce flow rate, the impedance during heating was normalized to a baseline value and the minimum rate of change in impedance, which occurred 1-2 s after heater activation, was recorded.

$NaH_2PO_4 \cdot H_2O$ in 1 L of double-distilled water [38]. The heater's DC resistance was measured using a Keithley 2400 SourceMeter and electrochemical impedance spectra was acquired between 1 Hz and 1 MHz using a Gamry R600 potentiostat. Fluidic testing was performed by flowing PBS through packaged sensors using a Watson Marlow 120U peristaltic pump with a flow rate range of 0 to 400 μL/min. Constant current pulses were delivered to the heater using a Keithley 2400 SourceMeter and electrochemical impedance was measured at 100 kHz and 1 V_{PP} using an Agilent E4980A LCR meter. Sensor performance was first characterized under static conditions using heater currents between 0.5 and 6 mA, corresponding to overheat temperatures between 0 and 9 °C, and was then characterized at flow rates between -400 and 400 μL/min using a 2 mA heater current. Sensors were also characterized in 0.25, 0.5, 1, and 2× dilutions of PBS, which have ionic concentrations of 0.07, 0.14, 0.28, and 0.56 mol/L respectively, as well as tap water. Additional characterization was performed in PBS at temperatures between 19 and 30 °C, with the exact temperature at the heater confirmed through measurement of the DC resistance of the heater.

To transduce flow velocity, the electrochemical impedance across a pair of sensing electrodes was recorded by a LabVIEW program at a rate of 5 Hz. The baseline impedance without heating was measured, and any deviations from this baseline due to heating were normalized as a percent change. The instantaneous rate of change was then calculated while the heater was active, and the minimum rate of change, corresponding to the fastest increase in temperature at the electrodes, was taken as a measurement of the flow velocity (Figure 6).

VI. Results

Characterization of the electrodes at different temperatures showed that the largest temperature-based changes in electrochemical impedance occurred at frequencies greater than ~60 kHz, corresponding to the frequency range at which phase approaches zero. To ensure that all measurements were in this range, all impedance measurements were performed at 100 kHz. Heater characterization showed that the TCR of

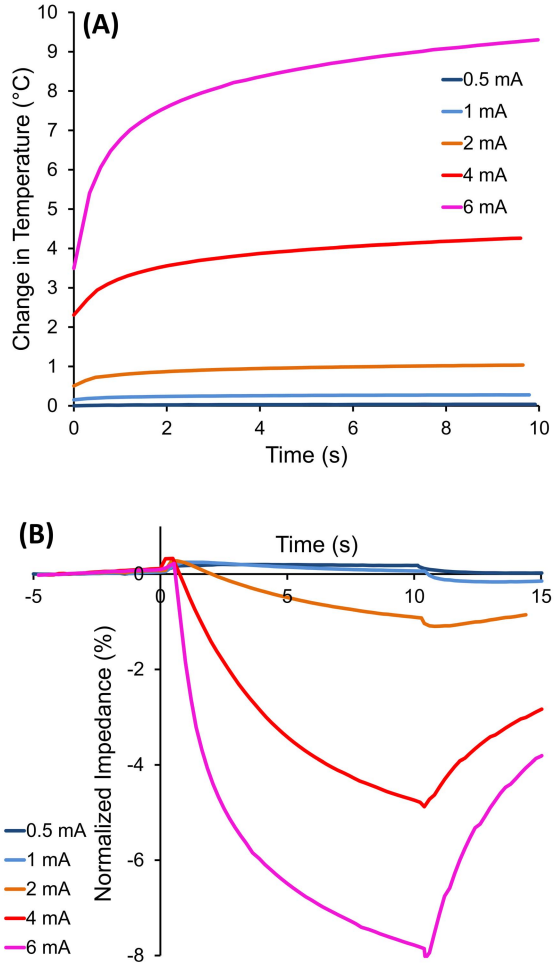

Fig. 7. (A) The overheat temperatures at the heater and (B) the response of an electrode pair 1 mm away for various current levels at no flow.

the resistive heater was approximately 0.16 %/°C, which is within the expected range for thin-film platinum [39]. From the TCR, the overheat temperature was calculated during flow testing by recording the heater's resistance during current injections. Figure 7 shows the heater overheat temperature and the impedance of electrodes 1 mm away normalized to the pre-heating value. A heater current of 2 mA provided an adequate impedance response with an overheat temperature of only 1.04 °C. To minimize power consumption and reduce the risk of damaging tissue or other structures due to excessive heating, all subsequent tests used a heater current of 2 mA.

A volumetric flow rate of 1 μL/min will result in a flow velocity of 2 μm/s when sent through a tube with a diameter of 3.25 mm. Figure 8A shows the impedance response of electrodes 1 mm away from the heater operating at an overheat temperature of 1°C under different flow velocities. The response profile and the minimum rate of change of impedance was found to vary with flow velocity and to be consistent across multiple trials (Figure 8B).

Figure 9 shows the minimum rate of change of impedance at flow velocities between −800 and 800 μm/s. The rate of change versus flow velocity takes the form of a steadily increasing curve at small negative and positive flow velocities, but begins to level off at large negative flow velocities. The

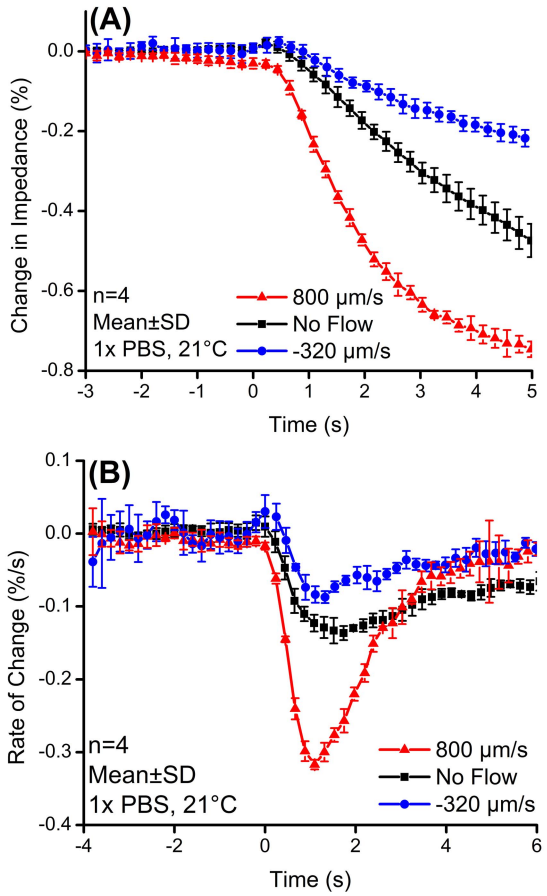

Fig. 8. (A) The percent change in impedance at electrodes 1 mm away from heater during constant 1°C heating and (B) the instantaneous rate of change. The minimum (peak) of the rate of change is used to transduce flow velocity.

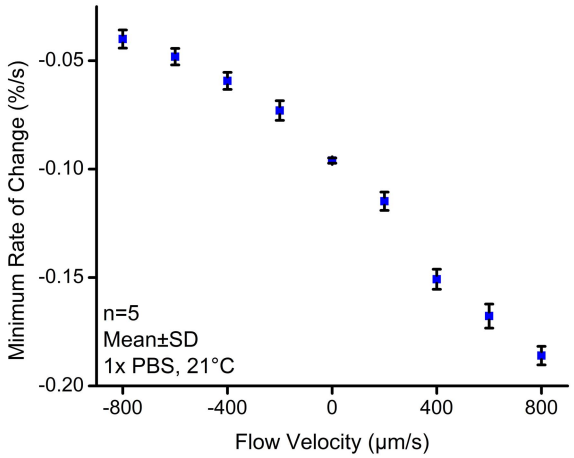

Fig. 9. The minimum rate of change of impedance 1 mm away at flow velocities from −800 to 800 μm/s.

maximum standard deviation between −200 and 200 μm/s is 43.3 μm/s.

Figure 10 shows the response of sensors with electrodes spaced 0.5, 1, and 2 mm away from the heater. Changing the heater-electrode spacing changes the dynamic range of the sensor, and electrodes spaced 0.5 mm away from the heater showed a higher dynamic range than the electrodes at 1 mm. However, measurements from electrodes at a 0.5 mm spacing

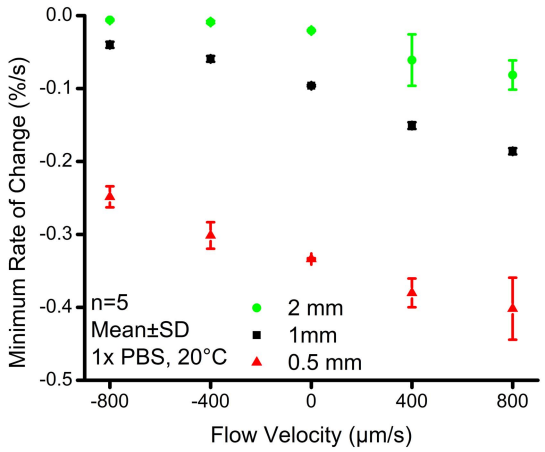

Fig. 10. The sensor response of electrodes spaced 0.5 mm, 1 mm, and 2 mm away from the heater. The response of electrodes at 4 mm was negligible.

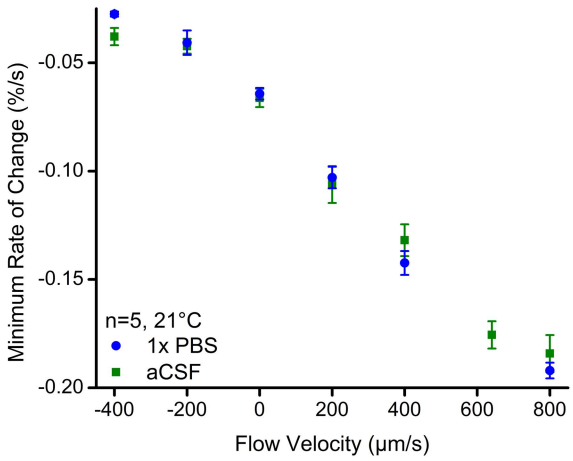

Fig. 11. A comparison of sensor response in 1x PBS and aCSF, which shows no significant differences.

were observed to be noisier than measurements at 1 mm. Sensors with a 4 mm electrode-heater spacing showed no response.

To ensure that results using PBS can be generalized to physiological fluids, a sensor was tested in both PBS and artificial cerebrospinal fluid (aCSF), which contains 150 mM Na^+, 3.0 mM K^+, 1.4 mM Ca^{2+}, 0.8 mM Mg^{2+}, 1.0 mM $PO4^{3-}$, and 155 mM Cl^-. Figure 11 shows the results, which reveal no significant differences in the response.

The baseline impedance of electrodes in different dilutions of PBS ranged from 3.67±0.04 kΩ in 2× PBS to 20.7±0.18 kΩ in 0.25× PBS, and electrodes in tap water showed a baseline impedance of 82.5±8.9 kΩ (n = 15, mean ± SD). Figure 12 shows the sensor's response in these solutions. As concentration decreased, the magnitude of the sensor's response increased slightly, though this change is only greater than standard deviation between tap water and the most concentrated PBS solution.

Figure 13 shows the sensor's response in 1× PBS at ambient fluid temperatures between 19 and 30°C. The baseline rate of change of the sensor decreases slightly over this range.

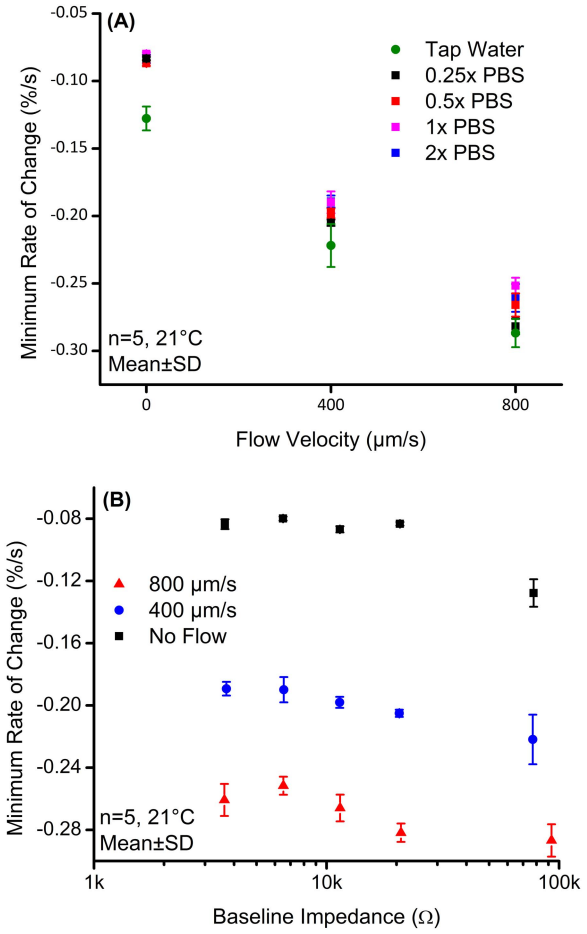

Fig. 12. (A) The minimum rate of change versus flow velocity at various dilutions of PBS. 0.25, 0.5, 1, and 2× PBS have ionic concentrations of 70, 140, 280, and 560 mM respectively. (B) The sensor response versus the baseline impedance of the temperature sensing electrodes.

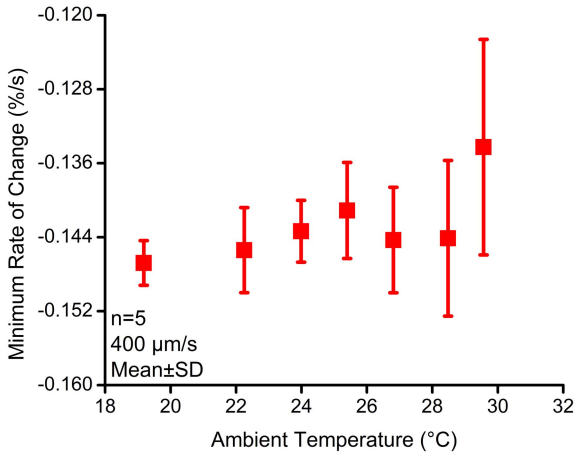

Fig. 13. The sensor response using 1°C overheat temperature at ambient temperatures between 19°C and 30°C. The minimum rate of change becomes slightly less sensitive at higher temperatures.

Using a 1°C overheat temperature is desirable to reduce power consumption and avoid tissue damage in *in vivo* applications, but higher overheat temperatures would provide greater dynamic range and potentially increase sensor resolution, which would be useful for non-implanted applications.

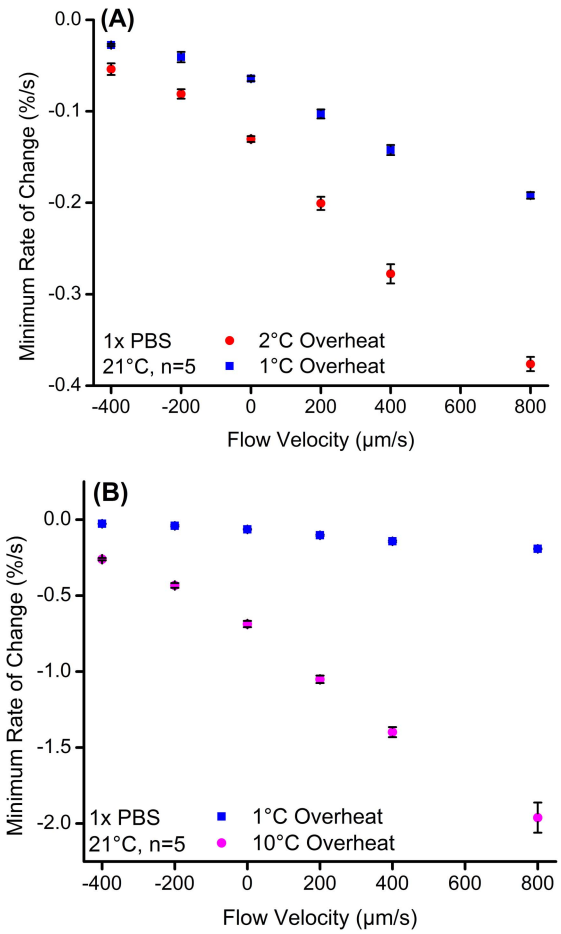

Fig. 14. Comparison of sensor response between (A) 1°C and 2°C and (B) 1°C and 10°C. Higher overheat temperatures are somewhat noisier but possess a significantly higher dynamic range, resulting in a net improvement in measurement resolution.

A sensor was characterized using a 1, 2, and 10 °C overheat temperatures, which correspond to 2, 2.9, and 6.2 mA currents delivered to the resistive heater. Figure 14 shows the sensor response results at these different operating regimes. When the overheat temperature is increased from 1 to 2 °C, the resolution improves significantly, with the standard deviation between −200 and 200 μm/s decreasing from 28.6 to 17.3 μm/s. Increasing the overheat temperature to 10 °C further decreases the resolution to 13.1 μm/s, though this improvement is not proportional to the change in temperature due to higher measurement variations seen during higher temperature operation.

VII. Discussion

Results from sensor testing matched simulation results in that the maximum rate of change of temperature at downstream electrodes, which corresponded to the minimum rate of change of impedance, can be used to transduce flow velocity (Fig. 15). However, experimental results showed a significantly lower dynamic range compared to the simulation, most likely due to heat loss through the walls of the luer lock connector, which assumed to be zero in the simulation. At negative and low positive velocities, the minimum rate of change was related to flow velocity as predicted by the

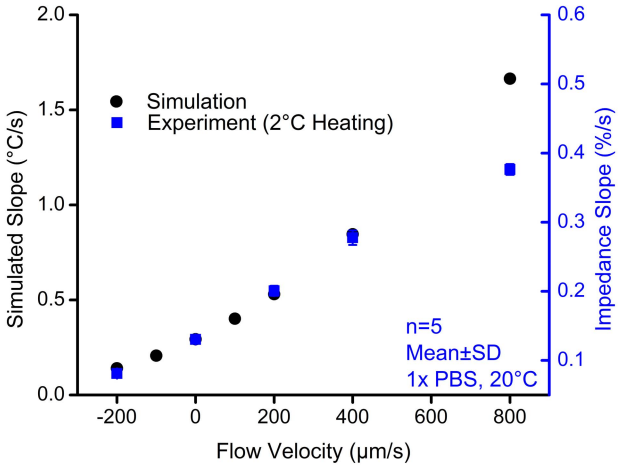

Fig. 15. A comparison between simulated results and experimental results, both with approx. 2°C heating. The results show a similar pattern over the majority of flow rates, though due to heat loss through the walls of the flow channel the experimental results have a lower dynamic range.

simulation, but at high positive velocities the rate of change began to deviate slightly from what the simulation predicted. This may have been due to the use of constant current to heat the fluid, which would result in a small decrease in heater temperature as the flow velocity increases. The dynamic range at higher flow velocities could therefore be improved by using a constant temperature at the resistive heater, though this would necessitate more complex feedback circuitry.

The decrease in sensor response with both increasing ambient temperature and increasing ionic concentration also followed theoretical predictions, although the changes in sensitivity with ionic concentration were found to be insignificant within an order of magnitude difference in ionic concentration. However, when used in an environment where large changes in ionic concentration are expected, the baseline impedance of the sensing electrodes without heater activation could be used to calibrate sensor response, though this would require *a priori* calibration over the expected ionic concentration range. Changes in sensitivity with ambient temperature were small but significant compared to the sensor's dynamic range for future applications, the heating resistor may be used as an ambient temperature sensor for real-time calibration, since the resistance of platinum is highly stable and increases linearly with temperature. Similar devices were fabricated which used a second platinum resistor as a temperature sensor, but after initial testing these were discarded due to the low TCR of the resistor and inductive coupling between the heater and resistor, which overwhelmed any flow-based effects.

The dynamic range of the sensor was relatively small when using a 1 °C overheat temperature, but was improved during operation with 2 and 10 °C overheat temperature. Slightly increasing the overheat temperature result in noticeable improvements in sensor resolution, and for *ex vivo* applications, overheat temperatures even higher than 10 °C may be useful, as long as those temperatures do not affect the surrounding environment. Association for the Advancement of Medical Instrumentation standards limit temperature increases in implants to between 1 and 2 °C [40], so any implantable device will need to stay within this range, but even with a minimal overheat temperature, the sensor can transduce flow velocity ranges relevant to cerebrospinal fluid flow through hydrocephalus shunts [41] or external ventricular drains [42] as well as capillary blood flow [43]. Arterial blood flow has a much higher average velocity, but even without increasing overheat temperature, the sensor can be tailored to measure higher flows by increasing the distance between electrode and heater. Multiple pairs of electrodes could also be used to transduce a wider range of flow velocities. Outside of the body there are many applications from cell culturing to microfluidic diagnostics that could benefit from low flow rate sensing of electrolytic solutions. Furthermore, benchtop devices could have higher operating temperature limits compared to *in vivo* applications and could therefore be tuned to a much wider range of flow velocities.

The small size of our sensor and its construction on a flexible substrate allow it to be easily integrated into shunts, catheters, and other equipment, and this design could be further miniaturized to access additional applications. Future work will investigate changing the size and orientation of electrodes in order to improve sensitivity and the use of calorimetric sensing to obtain a larger measurement range and decrease the time per measurement. Future work will focus on reducing measurement variation in order to improve resolution. This variation was observed to be much smaller when the sensor was tested without flow compared to when fluid was flowing, indicating that the pulsatile operation of the pump may be reflected in the sensor's output. The sensor may also move when subjected to flow, as only one end of the sensor is affixed to the wall of the luer lock connector; this movement may further contribute to measurement variation. Variation between devices was also present, which may have been a result of small deviations in the placement of the Parylene sensor die from the center of the flow channel. Non-centered placement of the sensor would result in a lower flow velocity at the sensor die, which may have caused a baseline shift. Before packaging an assumption was made that, due to water's high thermal conductivity, heat would spread to the region of highest flow velocity quickly enough that small deviations from center would not have a noticeable effect on sensor performance. Future work will test this assumption and evaluate whether an alternative packaging scheme could decrease inter-device variability.

Table 2 shows select parameters of several commercial and laboratory flow sensors. ΔT is the overheat temperature used and range is either the total range over which effective flow measurements can be made or the largest range tested, whichever is smaller. Resolution for commercial sensors is usually defined as 3$\times$ the standard deviation, but in literature the value usually reported is the smallest flow rate difference at which a difference in measurements was detected. There are very few commercial thermal flow sensors which are able to sense liquids traveling at low flow velocities, and of these the Sensirion sensor is the most effective, reporting a minimum detectable flow velocity of $\sim$14 μm/s with a very wide detectable flow range. However, all available commercial liquid flow sensors use silicon-based sensing elements and

TABLE II
A COMPARISON OF SEVERAL THERMAL FLOW SENSORS, BOTH COMMERCIAL AND REPORTED IN LITERATURE

	Sensing Method	Substrate Material	ΔT (°C)	Resolution (μm/s)	Range (mm/s)
Sensirion SLI-0430 [4]	—	Silicon	—	13.8	±9.2
POSiFA PTFD10 [5]	Calorimetric	Silicon	65	—	0-1850
Ashauer 1998 [7]	Time of Flight	Silicon, SiN	14	100	0-140
Wu 2001 [8]	Anemometer	Silicon, PSG	13	1670	0-66.7
Meng 2008 [10]	Time of Flight	Parylene C	24	10.4	0-0.6
Ahrens 2009 [14]	Anemometer	Polyimide	12	2890	0-57.9
Vilares 2010 [16]	Calorimetric	SU-8	60	66.7	±41.7
This Work	Time of Flight	Parylene C	1	43.3	±0.8

high overheat temperatures, rendering them incompatible with chronic *in vivo* use. Many other thermal flow sensors designed for water or other liquids have been reported in literature, but these have high overheat temperatures, low sensitivities, or non-biocompatible materials which prevent their use *in vivo*.

VIII. CONCLUSION

A thermal flow sensor which uses electrochemical impedance to measure changes in temperature was designed and tested. The use of impedance as well as a novel time of flight method for transducing flow allows for bidirectional measurement of low flow velocities with an overheat temperature of only 1°C. Accurate flow transduction is possible despite variations in ionic concentration, and in-use temperature calibration is possible thanks to the use of a platinum resistive heater. Due to its flexible, robust, and biocompatible design this sensor is useful in a wide range of applications for which current thermal flow sensors are not suitable, including chronic implantation in the human body

ACKNOWLEDGMENT

The authors would like to thank Madelina Pratt and Willa Jin for their help with characterization and testing and Dr. Brian Kim and the members of the Biomedical Microsystems Laboratory of USC for all of their help and support.

REFERENCES

[1] J. T. W. Kuo, L. Yu, and E. Meng, "Micromachined thermal flow sensors—A review," *Micromachines*, vol. 3, no. 3, pp. 550–573, 2012.
[2] J. J. Barron and C. Ashton, "The effect of temperature on conductivity measurement," in *Proc. TSP*, vol. 7. 2005, pp. 1–6.
[3] S. B. Baumann, D. R. Wozny, S. K. Kelly, and F. M. Meno, "The electrical conductivity of human cerebrospinal fluid at body temperature," *IEEE Trans. Biomed. Eng.*, vol. 44, no. 3, pp. 220–223, Mar. 1997.
[4] *SLI Liquid Flow Meter Series*, Sensirion, Staefa ZH, Switzerland, 2015.
[5] *PTFD10 Thermal Flow Sensor Die*, I. POSiFA Microsyst., San Jose, CA 2016.
[6] N. T. Nguyen, "Micromachined flow sensors—A review," *Flow Meas. Instrum.*, vol. 8, pp. 7–16, Mar. 1997.
[7] M. Ashauer, H. Glosch, F. Hedrich, N. Hey, H. Sandmaier, and W. Lang, "Thermal flow sensor for liquids and gases," in *Proc. 11th Annu. Int. Workshop Micro Electro Mech. Syst. (MEMS)*, Jan. 1998, pp. 351–355.
[8] S. Wu, Q. Lin, Y. Yuen, and Y.-C. Tai, "MEMS flow sensors for nano-fluidic applications," *Sens. Actuators A, Phys.*, vol. 89, pp. 152–158, Mar. 2001.
[9] T. K. Hsiai *et al.*, "Micro sensors: Linking real-time oscillatory shear stress with vascular inflammatory responses," *Ann. Biomed. Eng.*, vol. 32, pp. 189–201, Feb. 2004.
[10] E. Meng, P.-Y. Li, and Y.-C. Tai, "A biocompatible parylene thermal flow sensing array," *Sens. Actuators A, Phys.*, vol. 144, pp. 18–28, May 2008.
[11] F. Kohl *et al.*, "A micromachined flow sensor for liquid and gaseous fluids," *Sens. Actuators A, Phys.*, vol. 41, pp. 293–299, Apr. 1994.
[12] A. Glaninger, A. Jachimowicz, F. Kohl, R. Chabicovsky, and G. Urban, "Wide range semiconductor flow sensors," *Sens. Actuators A, Phys.*, vol. 85, pp. 139–146, Aug. 2000.
[13] H. Ernst, A. Jachimowicz, and G. A. Urban, "High resolution flow characterization in Bio-MEMS," *Sens. Actuators A, Phys.*, vol. 100, no. 1, pp. 54–62, 2002.
[14] R. Ahrens and K. Schlote-Holubek, "A micro flow sensor from a polymer for gases and liquids," *J. Micromech. Microeng.*, vol. 19, no. 7, p. 074006, 2009.
[15] T. S. J. Lammerink, N. R. Tas, M. Elwenspoek, and J. H. J. Fluitman, "Micro-liquid flow sensor," *Sens. Actuators A, Phys.*, vols. 37–38, pp. 45–50, Jun./Aug. 1993.
[16] R. Vilares *et al.*, "Fabrication and testing of a SU-8 thermal flow sensor," *Sens. Actuators B, Chem.*, vol. 147, no. 2, pp. 411–417, Jun. 2010.
[17] A. Vanhoestenberghe and N. Donaldson, "Corrosion of silicon integrated circuits and lifetime predictions in implantable electronic devices," *J. Neural Eng.*, vol. 10, no. 3, p. 031002, Jun. 2013.
[18] S. Shibata, Y. Niimi, and M. Shikida, "Flexible thermal MEMS flow sensor based on Cu on polyimide substrate," in *Proc. IEEE SENSORS*, Nov. 2014, pp. 424–427.
[19] C. Li, P.-M. Wu, J. A. Hartings, Z. Wu, C. H. Ahn, and R. K. Narayan, "Cerebral blood flow sensor with *in situ* temperature and thermal conductivity compensation," in *Proc. IEEE 25th Int. Conf. Micro Electro Mech. Syst. (MEMS)*, Jan./Feb. 2012, pp. 1021–1024.
[20] H. Yu, L. Ai, M. Rouhanizadeh, D. Patel, E. S. Kim, and T. K. Hsiai, "Flexible polymer sensors for *in vivo* intravascular shear stress analysis," *J. Microelectromech. Syst.*, vol. 17, pp. 1178–1186, Oct. 2008.
[21] C. Li, P.-M. Wu, J. Han, and C. H. Ahn, "A flexible polymer tube lab-chip integrated with microsensors for smart microcatheter," *Biomed. Microdevices*, vol. 10, no. 5, pp. 671–679, 2008.
[22] R. A. Robinson and R. H. Stokes, *Electrolyte Solutions*. Mineola, New York, NY, USA: Courier Corporation, 2002.
[23] M. Berkowitz and W. Wan, "The limiting ionic conductivity of Na^+ and Cl^- ions in aqueous solutions: Molecular dynamics simulation," *J. Chem. Phys.*, vol. 86, no. 1, pp. 376–382, 1987.
[24] R. Zwanzig, "Dielectric friction on a moving ion. II. Revised theory," *J. Chem. Phys.*, vol. 52, no. 7, pp. 3625–3628, 1970.
[25] M. L. Huber *et al.*, "New international formulation for the viscosity of H_2O," *J. Phys. Chem. Ref. Data*, vol. 38, no. 2, pp. 101–125, 2009.
[26] H. J. Liebe, G. A. Hufford, and T. Manabe, "A model for the complex permittivity of water at frequencies below 1 THz," *Int. J. Infr. Millim. Waves*, vol. 12, no. 7, pp. 659–675, 1991.
[27] W. J. Ellison, "Permittivity of pure water, at standard atmospheric pressure, over the frequency range 0–25 THz and the temperature range 0–100 °C," *J. Phys. Chem. Ref. Data*, vol. 36, no. 1, pp. 1–18, 2007.
[28] L. Onsager, "Theories of concentrated electrolytes," *Chem. Rev.*, vol. 13, no. 1, pp. 73–89, 1933.

[29] E. R. Kandel, J. H. Schwartz, T. M. Jessell, S. A. Siegelbaum, and A. J. Hudspeth, *Principles of Neural Science*, vol. 4. New York, NY, USA: McGraw-Hill, 2000.
[30] C. Waymouth, "Osmolality of mammalian blood and of media for culture of mammalian cells," *In Vitro*, vol. 6, no. 2, pp. 109–127, 1970.
[31] T. Stocker, *Introduction to Climate Modelling*. Berlin, Germany: Springer, 2011.
[32] R. Goldstein, *Fluid Mechanics Measurements*. Boca Raton, FL, USA: CRC Press, 1996.
[33] E. Majchrzak, "The finite difference method for transient convection-diffusion problems," *Sci. Res. Inst. Math. Comput. Sci.*, vol. 11, no. 1, pp. 63–72, 2012.
[34] *SCS Parylene Properties*, Specialty Coat. Syst., Indianapolis, IN, USA, 2014.
[35] L. Yu, C. A. Gutierrez, and E. Meng, "An electrochemical microbubble-based MEMS pressure sensor," *J. Microelectromech. Syst.*, vol. 25, no. 1, pp. 144–152, 2016.
[36] B. J. Kim, W. Jin, L. Yu, and E. Meng, "MEMS electrochemical patency sensor for detection of hydrocephalus shunt obstruction," in *Proc. 28th IEEE Int. Conf. Micro Electro Mech. Syst. (MEMS)*, Jan. 2015 pp. 662–665.
[37] E. Meng, X. Zhang, and W. Benard, "Additive processes for polymeric materials," in *MEMS Materials and Processes Handbook*. Berlin, Germany: Springer, 2011, pp. 193–271.
[38] *Preparation of Artificial CSF*, Alzet Osmotic Pumps, Cupertino, CA 2016.
[39] F. Mailly *et al.*, "Anemometer with hot platinum thin film," *Sens. Actuators A, Phys.*, vol. 94, pp. 32–38, Oct. 2001.
[40] P. D. Wolf, "Thermal considerations for the design of an implanted cortical brain-machine interface (BMI)," in *Indwelling Neural Implants: Strategies for Contending With the In Vivo Environment*, W. M. Reichert, Ed. Boca Raton, FL, USA: CRC Press, 2008.
[41] M. Hara, C. Kadowaki, Y. Konishi, M. Ogashiwa, M. Numoto, and K. Takeuchi, "A new method for measuring cerebrospinal fluid flow in shunts," *J. Neurosurgery*, vol. 58, no. 4, pp. 557–561, 1983.
[42] J. M. Drake, C. Sainte-Rose, M. DaSilva, and J.-F. Hirsch, "Cerebrospinal fluid flow dynamics in children with external ventricular drains," *Neurosurgery*, vol. 28, pp. 242–250, 1991.
[43] E. N. Marieb and K. Hoehn, *The Cardiovascular System: Blood Vessels*, 9th ed. Pearson Education, Inc., New York, NY, USA, 2013.

Alex Baldwin received the B.S. degree in electrical engineering from the University of Arkansas, Fayetteville, in 2013, and the M.S. degree in biomedical engineering from the University of Southern California in 2015, where he is currently pursuing the Ph.D. degree in biomedical engineering with the Biomedical Microsystems Laboratory. He is a recipient of the USC Graduate School Fellowship. He is currently working on implantable physiological sensors constructed using polymer micromachining.

Lawrence Yu received the B.S. degree in biomedical engineering, M.S. degree in electrical engineering, and Ph.D. degree in biomedical engineering from the University of Southern California in 2009, 2010, and 2016, respectively. His work in the Biomedical Microsystems Laboratory focused on the development of a sensor platform for *in vivo* applications. He was a recipient of the Walt Disney Foundation Scholarship and the Rose Hills Foundation Fellowship.

Ellis Meng (M'02–SM'09) received the B.S. degree in engineering and applied science and the M.S. and Ph.D. degrees in electrical engineering from the California Institute of Technology (Caltech), Pasadena, in 1997, 1998, and 2003, respectively. She is currently a Professor and the Chair of the Department of Biomedical Engineering, University of Southern California, Los Angeles, where she has been since 2004. She also holds a joint appointment with the Ming Hsieh Department of Electrical Engineering. Her current research interests include bioMEMS, implantable biomedical microdevices, microfluidics, multimodality integrated microsystems, and packaging. She was the Viterbi Early Career Chair in the Viterbi School of Engineering. She is a member of Tau Beta Pi, the Biomedical Engineering Society, the Society of Women Engineers, and the American Society for Engineering Education. She was a recipient of the Intel Women in Science and Engineering Scholarship, the Caltech Alumni Association Donald S. Clark Award, and the Caltech Special Institute Fellowship. She has also received the NSF CAREER and Wallace H. Coulter Foundation Early Career Translational Research Awards. In 2009, she was recognized as one of the TR35 Technology Review Young Innovators under 35.